JOURNAL OF AGRICULTURAL AND FOOD CHEMISTRY

Purification of Antifreeze Protein from Wheat Bran (*Triticum aestivum* L.) Based on Its Hydrophilicity and Ice-binding Capacity

CHAO ZHANG,[†,‡] HUI ZHANG,*[,†,‡] LI WANG,[†] JUNHUI ZHANG,[†] AND HUIYUAN YAO[†]

State Key Laboratory of Food Science and Technology, Jiangnan University, 1800 Lihu Avenue, Wuxi 214122, China, and School of Food Science and Technology, Jiangnan University, 1800 Lihu Avenue, Wuxi 214122, China

Wheat-bran (*Triticum aestivum* L.) antifreeze protein (*Ta*AFP) was purified 323-fold to electrophoretic homogeneity with an overall yield of 1.64% from wheat-bran protein by a specific three-step procedure. The three-step procedure was quicker, cheaper, and more effective than the five-step procedure we used earlier. First, *Ta*AFP was concentrated by a phosphate buffer, on the basis of its strong hydrophilicity that was validated by thermal gravimetric analyses and a surface hydrophobicity analysis. Second, *Ta*AFP was trapped in ice crystals for its specific ice-binding capacity, which was proved by ice-binding protocols. Remarkably, the ice-binding step was the most effective step, and the purification factor of this step was up to 270-fold. Finally, *Ta*AFP was purified by HPLC purification, a complementary step for the specific ice-binding protocol, to electrophoretic homogeneity. Our protocols provide peers a novel and effective way for the search and purification of potential AFPs.

KEYWORDS: Antifreeze protein; hydrophilicity; ice binding; wheat bran; purification; thermal hysteresis; surface hydrophobicity

INTRODUCTION

Antifreeze protein (AFP) is a kind of protein that decreases the freezing point noncolligatively, referred to as thermal hysteresis activity (THA), and retards recrystallization strongly (*1*). AFPs found in various organisms, including polar fish, cold-adapted insects, cold-induced plants, polar bacteria, and so forth, have remarkably diverse structures (*2, 3*). However, these AFPs share strong hydrophilic and ice-binding capacities (*4, 5*) on the basis of their specific affinity to ice (*6*). Once bound to ice, AFPs lower the local freezing point in a noncolligative manner, by forcing ice to grow in curved fronts between the bound AFP molecules (*7*). The additional local curvature of the ice front makes further ice growth thermodynamically unfavorable, and thus ice is stabilized in its supercooling condition. However, if the temperature is further lowered, the threshold is reached where the energetic barrier no longer prevents ice growth over AFPs, and AFPs are trapped in ice (*8, 9*). On the other hand, the ice-binding of AFPs on a single ice crystal has previously been used to determine the different ice-binding planes of these diverse AFPs (*10*). In our study, the goal is to recover and trap AFP in ice, instead of it being used as an indicator of the ice-binding plane. Therefore, we use a random, multicrystalline ice nucleation with a temperature gradient condition to trap AFP in the entire ice surface and exclude non-AFP and solutes.

In our previous study, a novel wheat-bran (*Triticum aestivum* L.) AFP (*Ta*AFP) was purified 357-fold to electrophoretic homogeneity with an overall yield of 1.60% from wheat-bran protein by five successive and traditional steps (*11*). In order to simplify the procedure, we attempted to purify *Ta*AFP by trapping it in ice on the basis of its specific ice-binding capacity. Moreover, the hydrophilic and ice-binding capacities of *Ta*AFP were measured to ensure the feasibility, because *Ta*AFP was a new AFP and its properties were not known yet. On the other hand, our protocol gave peers a novel and effective way to search for new AFPs or purify AFPs.

MATERIALS AND METHODS

Preparation of Carrot (*Daucus carota*) AFP and *Ta*AFP. Carrot (*Daucus carota*) AFP (*Dc*AFP) and *Ta*AFP were prepared by the methods described earlier (*5, 11, 12*). The protein content was assayed by a Modified Lowry Protein Assay kit (Pierce Biotechnology Inc., Rockford, IL) following the instructions of the manufacturer. Bovine serum albumin (BSA) was used as a standard protein.

Determination of Hydrophilicity by Thermal Gravimetric Analysis Method. The hydrophilicity of the samples was assayed by a thermal gravimetric analysis (TGA) method, which reflected the hydrophilic affinity of the samples. Aliquots of 20 μL of the sample, including BSA, *Dc*AFP, or *Ta*AFP solutions with 10% (w/v) protein content, were heated from 30 to 400 °C at rate of 15 °C/min and with a nitrogen flow of 40 mL/min in 70 μL ceramic pans (TGA/SDTA 851^e, Mettler-

* Author to whom correspondence should be addressed. Tel. and Fax: +86-510-85919101. E-mail: loszc@hotmail.com.
† State Key Laboratory of Food Science and Technology.
‡ School of Food Science and Technology.

10.1021/jf0715065 CCC: $37.00
Published on Web 08/23/2007

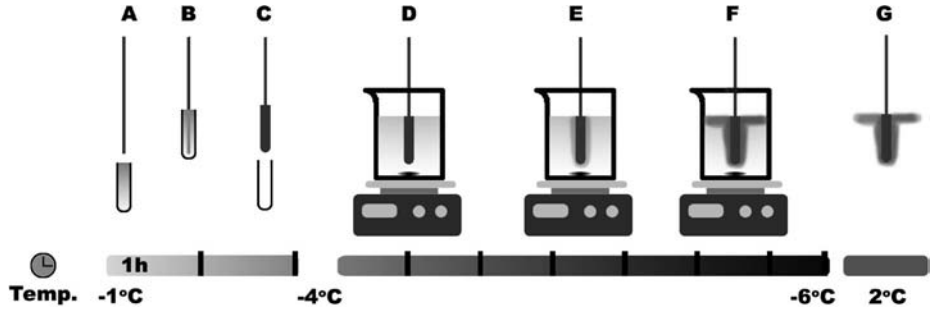

Figure 1. General ice-binding protocol. (A–C) Formation of the nuleator from −1 to −4 °C over 2 h; (C) nuleator; (D–F) ice-binding procedure, magnetic stirring slowly in the beaker from −4 to −6 °C for 7 h; (G) melting of the ice fraction at 2 °C. The lower bar shows both the time and temperature of the protocol.

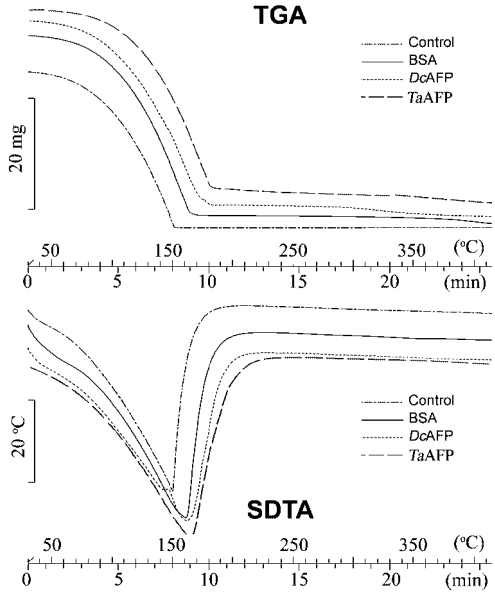

Figure 2. TGA and SDTA profiles of the control, BSA, *Dc*AFP, and *Ta*AFP solutions. Samples are heated from 30 to 400 °C at rate of 15 °C/min and with a nitrogen flow of 40 mL/min. TGA profiles show the weight loss during heating. SDTA profiles give the temperature difference between the cell and sample.

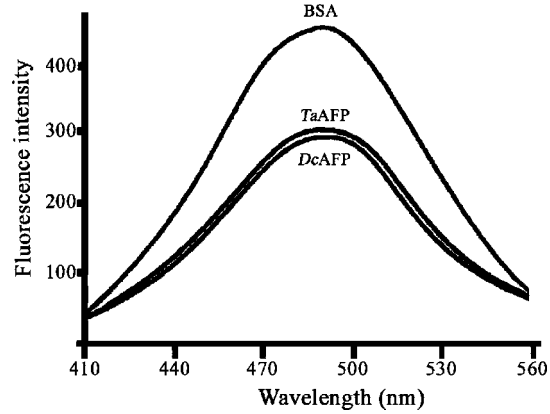

Figure 3. Fluorescence intensity profiles of BSA, *Dc*AFP, and *Ta*AFP solutions. Fluorescence intensity is measured with a fluorescence spectrometer at an excitation wavelength of 375 nm and an emission wavelength from 410 to 560 nm.

Toledo, Switzerland) (*13*, *14*). Double-distilled water was used as the control. The TGA profile shows the weight loss during heating. A synchronal differential temperature analysis (SDTA) profile gives the temperature difference between the cell and sample.

Determination of Surface Hydrophobicity by 1-Anilino-8-naphtalene-sulfonate Assay. The surface hydrophobicity of the samples was measured according to the methods described earlier (*15*, *16*) using fluorescent probe 1-anilino-8-naphtalene-sulfonate (ANS), reflecting the surface hydrophilicity of samples. The sample was dissolved in a 10 mM phosphate buffer solution (PBS; pH 8.0) with a protein content of 1 mg/mL. An aliquot of 40 μL of 8.0 mM ANS was added to a 2 mL sample. Fluorescence intensity was measured with a fluorescence spectrometer (Perkin-Elmer 2000, Boston, MA) at an excitation wavelength of 375 nm. Emission spectra were scanned from 410 to 560 nm.

Distribution Factor (δ) Determined by Ice-Binding Protocols. The distribution factor (δ) shows the distribution of the sample in an ice fraction or in a liquid fraction during the formation of an ice–water mixture, reflecting the ice-binding capacity of sample. The delta was measured as described in the earlier method (*8*) with a few modifications by our protocol (**Figure 1**). The nucleator was formed in a tube with 10 mL of double-distilled water over 2 h at a temperature between −1 and −4 °C. Specifically, a stainless stick (Φ 6 × 250 mm) was immersed in a 25 mL centrifuge tube with 10 mL of double-distilled water frozen between −1 and −4 °C for 2 h. When frozen, the centrifuge tube was immersed in water for about 30 s at room temperature. Then, the nucleator could be taken out freely. Meanwhile, aliquots of 100 mg of the sample, including BSA, *Dc*AFP, or *Ta*AFP, were dissolved in 90 mL of 10 mM PBS (pH 8.0) followed by centrifugation at 3000*g* at 4 °C for 20 min. The supernatant was stirred at −4 °C slowly in a beaker. When the supernatant reached −4 °C, the nucleator was immersed in the breaker and was continually stirred slowly at a temperature gradient from −4 to −6 °C for 7 h. When the ice was about 40% of the volume of the original solution, the nucleator was removed from the beaker. The remaining unfrozen solution was denoted as a liquid fraction and the frozen ice as an ice fraction. After the removal of the nucleator from the liquid fraction, the nucleator was washed with about 10–20 mL of prechilled double-distilled water (< 0 °C) to remove any remaining liquid to the liquid fraction. The ice fraction and liquid fraction were lyophilized. The delta is the ratio of the protein weight of the ice fraction to the sum protein weight of the ice fraction and the liquid fraction, as shown in formula 1.

$$\sigma = \frac{m_I}{m_I + m_L} \times 100\% \quad (1)$$

where δ is the distribution factor, m_I is the protein weight of the ice fraction (mg), and m_L is the protein weight of the liquid fraction (mg).

Purification of *Ta*AFP on the Basis of its Hydrophilicity and Ice-Binding Capacities. A three-step procedure was done to purify *Ta*AFP from wheat-bran (*Triticum aestivum* L.) protein. Aliquots of 100 g of wheat bran were stirred in 400 mL of 10 mM PBS (pH 8.0) for 4 h at room temperature followed by centrifugation at 3000*g* and 4 °C for 20 min. The supernatant was subjected to prechilled conditions at −4 °C and was bound to the nucleator as described in the protocol above, denoted as round 1. The thawed ice fraction from round 1 was subjected to prechilled conditions at −4 °C and was bound to the nucleator again, denoted as round 2. Then, both the ice fraction and liquid fraction were lyophilized. The ice fraction, after round 2, was lyophilized and

Table 1. Distribution Factor (δ) of BSA, *Dc*AFP, and *Ta*AFP Solutions[a]

sample	process	ice fraction (mg)	liquid fraction (mg)	total protein (mg)	distribution factor (δ)
BSA	round 1	-	9.8 ± 0.2^{a}	10 ± 0.2^{a}	$2.0 \pm 0.2\%^{a}$
	round 2	-	9.4 ± 0.1^{b}	9.8 ± 0.2^{a}	$4.1 \pm 0.2\%^{b}$
*Dc*AFP	round 1	9.3 ± 0.1^{a}	-	10 ± 0.1^{a}	$93.0 \pm 0.1\%^{c}$
	round 2	8.6 ± 0.1^{b}	-	9.3 ± 0.2^{b}	$92.5 \pm 0.3\%^{c}$
*Ta*AFP	round 1	9.4 ± 0.2^{a}	-	10 ± 0.3^{a}	$94.0 \pm 0.3\%^{c}$
	round 2	8.7 ± 0.1^{b}	-	9.4 ± 0.1^{b}	$92.6 \pm 0.2\%^{c}$

[a] A dash (-) means not assayed. [b] Data are means $\pm$ standard deviation ($n = 3$). [c] Data in the same column with different letters as superscripts are significantly different ($P < 0.05$).

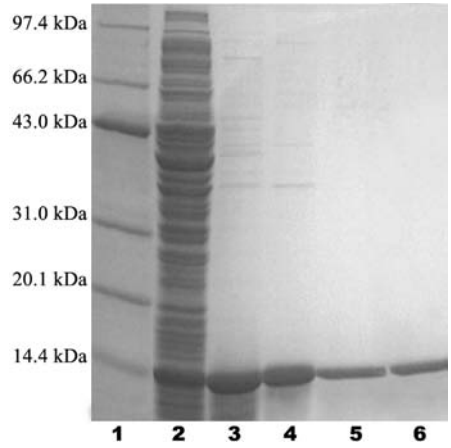

Figure 4. SDS-PAGE gel of a three-step procedure. Lane 1 is the low-molecular-weight marker including rabbit phosphorglase B (97.4 kDa), bovine serum albumin (66.2 kDa), rabbit actin (43.0 kDa), bovine carbonic anhydrase (31.0 kDa), trypsin inhibitor (20.1 kDa), and hen egg white lysozyme (14.4 kDa). Lane 2 is the crude extraction fraction. Lane 3 is the ice fraction after ice-binding protocols round 1. Lane 4 is the ice fraction after ice-binding protocols round 2. Lane 5 is the final *Ta*AFP after the three-step procedure. Lane 6 is the *Ta*AFP purified by a traditional five-step procedure (*11*).

subjected to high-performance liquid chromatography (HPLC) purification. The lyophilized sample was redissolved in 10 mM PBS (pH 8.0) with a protein content of 1 mg/mL. An aliquot of 5 μL of the sample was subjected to a Shodex PROTEIN KW-804 column (0.80 $\times$ 30 cm, Shodex, Showa Denko KK, Tokyo, Japan) at rate of 1.0 mL/min and eluted with a linear NaCl gradient (0–0.3 M) in 10 mM PBS (pH 8.0) for 30 min, with monitoring at 220 nm.

Electrophoresis. Sodium dodecyl sulfate polyacrylamide gel electrophoresis (SDS-PAGE) was done according to the system of Laemmli (*17*) with a few modifications (*18*). The sample was mixed at a 1:1 (v/v) ratio with the SDS-PAGE sample buffer (0.125 M Tris-HCl, pH 6.8, 10% SDS, 20% glycerol, 10% β-mercaptoethanol) and was boiled for 5 min. An aliquot of 10 μL of the sample was loaded into the gel made of 4% stacking and 12.5% separating gels and subjected to electrophoresis at a constant current of 15 mA per gel using a Mini-Protean III Cell apparatus (Bio-Rad Laboratories, Mississauga, ON). After electrophoresis, gels were stained with 0.1% Coomassie-Brilliant-Blue R-250 in 50% methanol and 7% acetic acid and destained with 7% acetic acid. The molecular weight of the sample's subunits was estimated by measuring their relative mobility in the SDS-PAGE gel, comparing with those of low-molecular-weight markers (Amersham Pharmacia Biotech): rabbit phosphorglase B (97.4 kDa), bovine serum albumin (66.2 kDa), rabbit actin (43.0 kDa), bovine carbonic anhydrase (31.0 kDa), trypsin inhibitor (20.1 kDa), and hen egg white lysozyme (14.4 kDa).

Determination of THA by the Differential Scanning Calorimeter Method. THA was measured by the differential scanning calorimeter (DSC) method reported earlier (*18, 19*). An aliquot of 10 μL of the sample was sealed in a preweighed aluminum pan and cooled from room temperature to -30 °C at rate of 3 °C/min and held for 15 min, followed by heating to 20 °C at a rate of 3 °C/min (Diamond DSC-7, Perkin Elmer Pyris, Boston, MA). The melting point (T_m) was calculated by Pyris Software for Windows, version 3.80. Then, the sample was cooled from +20 °C to -30 °C at rate of –3 °C/min, held for 15 min, and then heated to the holding temperature (T_h) when the system was at phase-equilibrium with the solid (ice crystal) and liquid (aqueous solution). After holding at T_h for 2 min, the sample was cooled from T_h to -30 °C at rate of –3 °C/min. The onset temperature (T_0) was recorded by Pyris Software for Windows, version 3.80. The process was repeated at different T_h. THA was calculated using formula 2. The calorimeter was temperature- and heat-calibrated with indium as a standard.

$$\mathrm{THA} = T_h - T_0 \quad (2)$$

where T_h is the holding temperature and T_0 is the onset temperature when the exothermic process begins.

Statistical Analysis. All data were expressed as the mean value $\pm$ standard deviation ($n \geq 3$). All statistical analyses were done with the Super ANOVA software (version 1.11, Abacus Concepts Inc., Berkeley, CA). One-way ANOVA and multiple comparisons (Fisher's least-significant difference test) were used to evaluate the significant differences of data at a criterion of $P < 0.05$.

RESULTS AND DISCUSSIONS

Strong Hydrophilicity and Weak Surface Hydrophobicity of *Ta*AFP. To prove its strong hydrophilicity, the hydrophilicity and surface hydrophobicity of *Ta*AFP were evaluated. The hydrophilicity of *Ta*AFP is evaluated by TGA and SDTA profiles (**Figure 2**). In TGA and SDTA profiles, the water of the sample will need a longer time to evaporate when the sample has strong hydrophilicity (*4*). Therefore, the sample that needs a longer time to lose its water has the stronger hydrophilicity (*4*). Specifically, the 90%-weight-loss temperature was monitored, because BSA, *Dc*AFP, and *Ta*AFP solutions all had 90% water. The hydrophilicity of the sample increased with the raising of the 90%-weight-loss temperature (*4, 5*). The 90%-weight-loss temperatures were 148, 168, 178, and 180 °C of the control, BSA, *Dc*AFP, and *Ta*AFP solutions, respectively. Moreover, *Dc*AFP and *Ta*AFP solutions showed higher 90%-weight-loss temperature than those of the control and BSA solution. Therefore, the hydrophilicity of the *Dc*AFP and *Ta*AFP solutions was stronger than that of the BSA solution. Furthermore, similar results were observed in SDTA profiles. The water evaporation of the control, BSA, *Dc*AFP, and *Ta*AFP solutions stopped at about 195, 206, 218, and 221 °C, respectively. The water of the *Dc*AFP and *Ta*AFP solutions needed a longer time to escape from the protein than those of the control and BSA solution. The water of the *Dc*AFP solution took more time to evaporate, as a result of its strong hydrophilicity, which had been proved in our previous study (*18*). On the other hand, Deng et al. pointed out that all AFPs have strong hydrophilicity (*20, 21*). Remarkably, the *Ta*AFP solution required a similar time to evaporate 90% of its weight as that of the *Dc*AFP solution, consistent with the results reported by Deng et al. (*20, 21*). Moreover, *Ta*AFP was a glycine-rich protein (*11*) that showed

Table 2. Summary of *Ta*AFP Purification from Wheat Bran

step		protein (mg)	THA (°C)	specific THA (°C/mg protein × 10^{-7})	yield (%)	purification factor
crude extract		5963	0.0032	5.37	100	1
ice-binding protocol	round 1	137	0.0168	1226.28	2.30	228.36
	round 2	116	0.0168	1448.28	1.95	269.70
HPLC analysis		98.0	0.0170	1734.69	1.64	323.03

strong hydrophilicity, as proved by hydropathy plots done earlier (*22*), confirming our result that *Ta*AFP had strong hydrophilicity.

The result of the surface hydrophobic assay by ANS analysis was similar to that of the TGA analysis (**Figure 3**). ANS analysis is a classical method to evaluate the surface hydrophobicity of a protein. This method is evaluated by its fluorescence intensity, reflecting the relative hydrophobic intensity of the sample. The higher the fluorescence intensity is, the stronger the surface hydrophobicity is (*15*, *16*). Specifically, the surface hydrophobicity of the BSA solution was stronger than that of the *Dc*AFP and *Ta*AFP solutions.

*Ta*AFP solution showed stronger hydrophilicity than BSA solutions, and weaker hydrophobicity than BSA solution. Therefore, *Ta*AFP had a strong hydrophilicity and strong affinity to water, similar to that of *Dc*AFP or other known AFPs.

Ice-Binding Capacity of *Ta*AFP. The distribution factor (δ) of the *Dc*AFP and *Ta*AFP solutions was measured by the ice-binding protocol (**Figure 1**) to evaluate the ice-binding capacity. In contrast, the BSA solution was assayed as the control at the same time. Supercooling and ovegrowth of the ice should be avoided in order to trap AFP in ice (*8*). In our protocol, supercooling and overgrowth of the ice was avoided by the following methods: (1) a lower sample content (1 mg/mL) to decrease the energy barrier and keep ice formation ongoing, (2) magnetic stirring to ensure the continuity of the liquid fraction, and (3) lowering of the temperature gradually to overrun the threshold and trap AFP. **Table 1** shows the distribution factor (δ) of BSA, *Dc*AFP, and *Ta*AFP solutions. The δ of the BSA solution was obviously lower than those of the *Dc*AFP and *Ta*AFP solutions. More than 90% of the *Dc*AFP and *Ta*AFP were bound to ice, proving that *Dc*AFP and *Ta*AFP had specific ice-binding capacities. Moreover, *Dc*AFP has strong hydrophilicity and can control the movement of freezable water content (*18*, *23*). Therefore, the specific ice-binding capacity of *Dc*AFP and *Ta*AFP solutions was confirmed. In conclusion, *Ta*AFP had a specific ice-binding capacity, similar to those of other known AFPs (*8*, *24–26*).

Purification of *Ta*AFP from Wheat-Bran Protein by a Three-Step Procedure. *Ta*AFP is purified 357-fold to electrophoretic homogeneity with an overall yield of 1.60% from wheat-bran protein in five-step procedures as described in our previous study (*11*). In this study, *Ta*AFP was purified to electrophoretic homogeneity on the basis of its specific hydrophilicity and ice-binding capacities. Meanwhile, the five-step procedure was reduced to three steps, including crude extraction, an ice-binding protocol, and HPLC purification. First, the crude extraction took full advantage of *Ta*AFP's specific hydrophilicity to dissolve in 10 mM PBS (pH 8.0) and separate easily from other components. Second, *Ta*AFP was trapped by ice on the basis of its specific ice-binding capacity by the ice-binding protocol. The purification factor was up to 270-fold. Therefore, the ice-binding protocol step was the most effective step in the three-step procedure. The purification factor of round 1 and round 2 was similar during the ice-binding protocol. Remarkably, the purity of *Ta*AFP was improved significantly in round 2 (**Figure 4**). Therefore, round 2 was an indispensable part of the three-step procedure. HPLC purification was an effective supplement of specific purification. In summary, *Ta*AFP was purified to electrophoretic homogeneity more quickly than the traditional method we used earlier (*11*). The three-step procedure was summarized in **Table 2**, showing that *Ta*AFP was purified 323-fold to electrophoretic homogeneity with an overall yield of 1.64 % from wheat-bran protein. In conclusion, the overall yield of the three-step procedure was a little higher than that of the five-step procedure. Nevertheless, the three-step procedure was simpler, more effective, and low-cost and can be applied to the search and purification of new AFPs.

ABBREVIATIONS

AFP, antifreeze protein; ANS, 1-anilino-8-naphtalene-sulfonate; BSA, bovine serum albumin; DcAFP, carrot (*Daucus carota*) antifreeze protein; DSC, differential scanning calorimeter; PBS, phosphate buffer solution; SDTA: synchronal differential temperature analysis; TaAFP, wheat-bran (*Triticum aestivum* L.) antifreeze protein; TGA, thermal gravimetric analyses; THA, thermal hysteresis activity.

LITERATURE CITED

(1) Knight, C. A.; Cheng, C. C.; DeVries, A. L. Adsorption of α-helical antifreeze peptides on specific ice crystal surface planes. *J. Biophys.* **1991**, *59*, 409–418.

(2) Ewart, K. V.; Lin, Q.; Hew, C. L. Structure, function and evolution of antifreeze proteins. *Cell. Mol. Life Sci.* **1999**, *55* (2), 271–283.

(3) Davies, P. L.; Baardsnes, J.; Kuiper, M. J.; Walker, V. K. Structure and function of antifreeze proteins. *Philos. Trans. R. Soc. London, Ser. B* **2002**, *357* (1423), 927–933.

(4) Wilson, P. W. A model for thermal hysteresis utilizing the anisotropic interfacial energy of ice crystals. *Cryobiology* **1994**, *31* (4), 406–412.

(5) Zhang, C.; Zhang, H.; Wang, L.; Yao, H. Validation of antifreeze properties of glutathione based on its thermodynamic characteristics and Baker's yeast protective ability during cryopreseration. *J. Agric. Food Chem.* **2007**, *55*, 4698–4703.

(6) Dalal, P.; Sonnichsen, F. D. Source of the ice-binding specificity of antifreeze protein type I. *J. Chem. Inf. Comput. Sci.* **2000**, *40* (5), 1276–1284.

(7) Wilson, S. L.; Kelley, D. L.; Walker, V. K. Ice-active characteristics of soil bacteria selected by ice-affinity. *Environ. Microbiol.* **2006**, *8* (10), 1816–1824.

(8) Kuiper, M. J.; Lankin, C.; Gauthier, S. Y.; Walker, V. K.; Davies, P. L. Purification of antifreeze proteins by adsorption to ice. *Biochem. Biophys. Res. Commun.* **2003**, *300* (3), 645–648.

(9) Du, N.; Liu, X. Y.; Hew, C. L. Ice nucleation inhibition - Mechanism of antifreeze by antifreeze protein. *J. Biol. Chem.* **2003**, *278* (38), 36000–36004.

(10) Miura, K.; Ohgiya, S.; Hoshino, T.; Nemoto, N.; Suetake, T.; Miura, A.; Spyracopoulos, L.; Kondo, H.; Tsuda, S. NMR analysis of type III antifreeze protein intramolecular dimer - Structural basis for enhanced activity. *J. Biol. Chem.* **2001**, *276* (2), 1304–1310.

(11) Zhang, C.; Zhang, H.; Wang, L.; Yao, H. Purification and characterization of a novel glycine-rich antifreeze protein from winter wheat-bran (*Triticum aestivum* L.). *Food Res. Int.* **2007**, Submitted.

(12) Smallwood, M.; Worrall, D.; Byass, L.; Elias, L.; Ashford, D.; Doucet, C. J.; Holt, C.; Telford, J.; Lillford, P.; Bowles, D. J. Isolation and characterization of a novel antifreeze protein from carrot (Daucus carota). *Biochem. J.* **1999**, *340*, 385–391.

(13) Riesen, R.; Vogel, K.; Schubnell, M. DSC by the TGA/SDTA851^e considering mass changes. *J. Therm. Anal. Calorim.* **2001**, *64*, 243–252.

(14) Soria, D. B.; Piro, O. E.; Castellano, E. E.; Aymonino, P. J. Crystal and molecular structure determination, TGA, DTA, and infrared and Raman spectra of rubidium nitroprusside monohydrate, $Rb_2[Fe(CN)_5NO]\cdot H_2O$. *J. Chem. Crystallogr.* **1999**, *29*, 75–80.

(15) Alizadeh-Pasdar, N.; Eunice, C. Y.; Li, C. Comparison of protein surface hydrophobicity measured at various pH values using three different fluorescent probe. *J. Agric. Food Chem.* **2000**, *48*, 328–334.

(16) Kato, A.; Nakai, S. Hydrophobicity determined by a fluorescence probe method and its correlation with surface properties of proteins. *J. Biochim. Biophys. Acta* **1980**, *624*, 13–20.

(17) Laemmli, U. K. Cleavage of structure proteins during the assembly of the head of bacteriophage T_4. *Nature* **1970**, *277*, 680–685.

(18) Zhang, C.; Zhang, H.; Wang, L. Effect of carrot (*Daucus carota*) antifreeze proteins on the fermentation capacity of frozen dough. *Food Res. Int.* **2007**, *40*, 763–769.

(19) Hansen, T. N.; Baust, J. G. Differential scanning calorimetric analysis of Tenebrio Molitor antifreeze protein-activity. *Cryobiology* **1988**, *25* (6), 525–526.

(20) Graham, L. A.; Liou, Y. C.; Walker, V. K.; Davies, P. L. Hyperactive antifreeze protein from beetles. *Nature* **1997**, *388* (6644), 727–728.

(21) Deng, G. J.; Andrews, D. W.; Laursen, R. A. Amino acid sequence of a new type of antifreeze protein: From the longhorn sculpin *Myoxocephalus octodecimspinosis*. *Febs Lett.* **1997**, *402* (1), 17–20.

(22) Kyte, J.; Doolittle, R. F. A simple method for displaying the hydropathic character of a protein. *J. Mol. Biol.* **1982**, *157*, 105–132.

(23) Meyer, K.; Keil, M.; Naldrett, M. J. A leucine-rich repeat protein of carrot that exhibits antifreeze activity. *Febs Lett.* **1999**, *447* (2–3), 171–178.

(24) Madura, J. D.; Baran, K.; Wierzbicki, A. Molecular recognition and binding of thermal hysteresis proteins to ice. *J. Mol. Recognit.* **2000**, *13* (2), 101–113.

(25) DeLuca, C. I.; Comley, R.; Davies, P. L. Antifreeze proteins bind independently to ice. *Biophys. J.* **1998**, *74* (3), 1502–1508.

(26) Verdier, J. M.; Ewart, K. V.; Griffith, M.; Hew, C. L. An immune response to ice crystals in North Atlantic fishes. *Eur. J. Biochem.* **1996**, *241* (3), 740–743.

Received for review May 22, 2007. Revised manuscript received July 21, 2007. Accepted August 2, 2007.

JF0715065